

A wideband lag correlator for heterodyne spectroscopy of broad astronomical and atmospheric spectral lines

A. I. Harris^{a)}

Department of Astronomy, University of Maryland, College Park, Maryland 20742

J. Zmuidzinas^{b)}

G. W. Downs Laboratory of Physics, California Institute of Technology, 320-47, Pasadena, California 91125

(Received 1 August 2000; accepted for publication 26 October 2000)

WASP2 is a lag correlation spectrometer that is optimized for astronomical heterodyne observations of spectral lines from mid-infrared through centimeter wavelengths. Since the instrument is a wideband microwave spectrum analyzer, its basic technology is well suited to radio astronomy, atmospheric remote sensing, and any other application which requires observations of broad spectral lines. In this specific instrument, eight 16 lag correlator boards form a 128 lag spectrometer with 33 MHz spectral resolution. The spectrometer's present microwave components dominate its gain shape, yielding a spectrometer which covers a useful (6 dB bandwidth) single band of 3600 MHz, from 280 to 3880 MHz. The correlator boards have a 3 dB bandwidth of 4000 MHz, from below 100 MHz to near their aliasing limit of 4200 MHz. WASP2 obtains its wide bandwidth with fully analog high frequency components: the voltage multipliers are transistor circuits and the delays are lengths of microstrip transmission line. WASP2 is simple, compact, requires little power, and integrates stably for many hours. © 2001 American Institute of Physics. [DOI: 10.1063/1.1334629]

I. INTRODUCTION

New astronomical and remote-sensing instruments require microwave spectrometers with modest spectral resolution over several gigahertz of instantaneous bandwidth. Applications include submillimeter and far-infrared observations of Doppler-broadened spectral lines from galaxies, millimeter-wave searches for distant objects with poorly known redshifts, and observations of pressure-broadened atmospheric lines. We have discussed some of these applications in more detail in an article that describes a prototype of our broadband spectrometer.¹

Here we describe WASP2 (wideband analog spectrometer), a second-generation broadband autocorrelation spectrometer with fully analog high frequency signal processing. Analog components allow a compact and simple system with low complexity and low power consumption. The spectrometer is small enough that it is easy to mount it on the telescope, very close to the receiver, simplifying the wideband connection between receiver and spectrometer. Although configured as a 128 channel autocorrelator, the spectrometer's correlator boards permit flexible spectrometer architectures with autocorrelation or cross correlation in any multiple of 16 lags. The basic WASP technology is consequently useful for either single-dish or interferometer array instruments. The WASP2 spectrometer contains eight of these correlator boards for 33 MHz resolution over a 6 dB bandwidth of 3600 MHz, providing resolution and bandwidth that are well matched to observations of distant galaxies at submillimeter wavelengths. In another instrument, a single correlator board

is the spectrometer in a 22 GHz water line radiometer that will make atmospheric phase corrections for interferometers.

WASP2 has several advantages over other types of spectrometers for many wideband applications. Compared with acousto-optical spectrometers, analog correlators have wider bandwidths by factors of 2–4. Compared with filter-bank spectrometers, most of WASP2's components are printed on or soldered to circuit boards, leading to an instrument which is considerably simpler, less massive, more compact, and which does not require high-tolerance machining. Compared with digital correlators, analog correlators eliminate high-speed digitization and digital signal processing, vastly reducing the instrument's power consumption and complexity. Analog delays and multiplications also do not degrade the signal to noise ratio with coarse digitization steps. Analog processing does have quirks. In particular, the sampling in time delay is not perfectly uniform and each sample has its own frequency response. Since sampling and other nonideal behavior is stable in time and can be accurately measured, these nonidealities do not significantly affect the spectrometer's performance, but only provide additional tasks for the data reduction software.

II. INSTRUMENT

A. Correlator cards

Autocorrelator spectrometers obtain spectra by using the Fourier transform relationship between a signal's autocorrelation function and power spectrum

$$S(f) = \int_{-\infty}^{\infty} R(\tau) \cos(2\pi f\tau) d\tau, \quad (1)$$

^{a)}Electronic mail: harris@astro.umd.edu

^{b)}Electronic mail: jonas@submm.caltech.edu

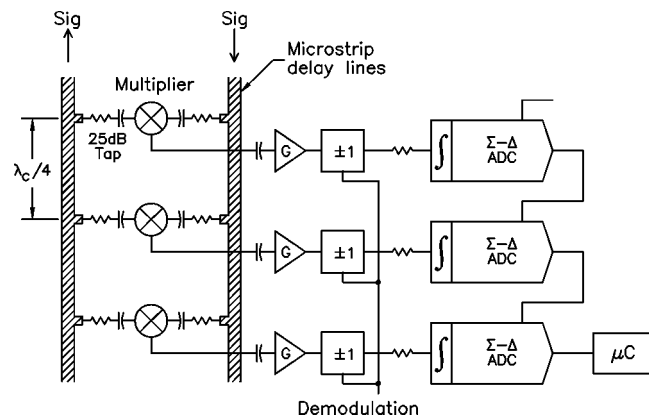


FIG. 1. Schematic view showing a section of the “ladder” of multipliers within WASP2 and its low-frequency signal processing electronics. Sections of microwave stripline provide propagation-time delays between fast transistor multipliers.

where $S(f)$ is the power spectrum as a function of frequency f and $R(\tau)$ is the signal’s autocorrelation function as a function of time delay (lag) τ . WASP2’s circuit boards contain all the components necessary to estimate the autocorrelation function

$$R(\tau) = \langle V(t)V(t+\tau) \rangle. \quad (2)$$

Tapped transmission lines provide the time delays τ , transistor multipliers form the product of the two input voltages $V(t)$ and $V(t+\tau)$, and low-frequency electronics integrate the multiplier output to provide the time average. Figure 1 is a schematic block diagram of the signal processing circuits contained on the correlator boards.

Nyquist sampling a band-limited signal requires measurement at a frequency at least twice the signal’s band-limited bandwidth Δf , or twice per shortest wavelength along a transmission line. Reflections between the taps of the tapped delay lines cause a strong, broad resonance when the wavelength is half the tap separation, however. The counter-propagating signals within WASP2 (Fig. 1) are delayed by equal amounts to each input, so the multipliers’ physical spacing at the Nyquist cutoff frequency f_c is a quarter wavelength along each line. With this geometry the resonance from tap reflections falls at twice the Nyquist cutoff frequency and does not degrade the response at the high end of the band.

A series of resistive power dividers sample the signal of a traveling wave along the transmission lines. Each sampling tap starts with a narrow (0.008 in.) trace extending from the line’s edge to an 820 Ω chip resistor, a direct current (dc) blocking capacitor, and then the multiplier input. Coupling to the multiplier is -24 dB at low frequencies, with the resistor’s shunt capacitance (~ 0.05 pF) increasing the coupling by a few decibels at the highest frequency. This rolloff is desirable, as it partially compensates for some of the multipliers’ rolloff with frequency. A Nyquist cutoff frequency $f_c = 4200$ MHz was chosen to match commercially available² broadband splitters;³ the corresponding tap spacing is 59.5 ps, or 0.380 in. along microstrip transmission lines on 0.020 in. thick $\epsilon_r = 3.5$ circuit board. Each line starts at a SMA end launch connector, continues through the 16 taps, and ends at

a chip resistor termination. The two transmission lines start at opposite ends of the circuit board, running close to the center along the long axis of the board. The inputs are well matched: peaks in the input return loss range from -20 to -15 dB across the spectrometer’s operating band.

The voltage multipliers are Agilent IAM-81008 active mixers.⁴ These MMIC devices have classical Gilbert multiplier cell cores⁵ and are good analog multipliers when local oscillator starved. Measurement of power linearity over a wide power range confirms that the devices match their theoretical response to input signals, $V_{\text{out}} = \alpha \tanh(\beta V_1 V_2)$, where α and β are unit-conversion constants. For this hyperbolic tangent saturation law the power gain compression factor is $f = (a/s_i) \tanh(s_i/a)$, where s_i is the input power and a is the saturation constant. With the measured value of $a = -17$ dB m, the 0.22 dB compression (5% deviation from linear) power is $s_i = -21$ dB m. For very high accuracy measurements, it is straightforward to correct for multiplier saturation in software.⁶ With a typical multiplier responsivity of 3 V/mW, -21 dBm corresponds to 24 mV at the multiplier’s output.

Amplification and demodulation precede each channel’s analog-to-digital converter (ADCs).⁷ Each ADC contains an internal analog integrator that integrates the signal over the spectrometer’s 11.5 ms readout cycle time. This ADC accepts bipolar inputs that in principle could match the autocorrelation function’s voltage range. Unfortunately, the ADC’s excess noise near zero volts in its bipolar mode precludes this, so circuitry after the hardware demodulators is needed to provide an offset to shift the bipolar correlation signal into positive voltages for unipolar analog to digital conversion. Switching the polarity of the phase switch signal (double phase switching) with each readout cycle and digital demodulation removes residual drift from this offset signal and restores the autocorrelation function’s bipolar range.

Autocorrelator electronics generally have higher dynamic range requirements than filter spectrometer electronics because the detectors see the entire input bandwidth instead of a filtered fraction. The radiometer equation gives the relationship between the maximum signal level, which is set by the receiver and input noise temperatures, and the minimum signal level, which is set by radiometric power fluctuations. The ratio of the two gives the minimum dynamic range for power measurements within the spectrometer:

$$\text{Dynamic range} = \frac{\bar{T}}{\Delta T_{\text{rms}}} = \sqrt{B \tau_{\text{int}}}. \quad (3)$$

For an autocorrelator this dynamic range requirement relaxes with increasing lag number because the noise level is approximately constant with lag but the magnitude of the correlated signal generally decreases. The input bandwidth B is set by the microwave components preceding the multiplier, and the analog integration time τ_{int} should be short enough to keep the dynamic range below a practical limit of 16 bits. For a rectangular 4000 MHz passband and WASP2’s 11.5 ms integration time, the dynamic range requirement is 6782 ($2^{12.7}$).

Electronic noise from the multipliers must be small compared with the radiometric fluctuations or the spectrometer will contribute significantly to the overall system noise. Audio frequency noise from the multipliers follows a $f^{-1.2}$ power spectrum with typical noise densities of 80–150 nV Hz $^{-1/2}$ at 1.5 kHz, dropping to a plateau at ~ 10 –20 kHz, and then continuing to drop as $\sim f^{-1}$ from 30 kHz to at least 100 kHz. Given the rather low output voltages from the multipliers when they are in their linear regimes, fast modulation and synchronous detection are necessary to reach sufficiently low noise levels. Correlation spectrometers can phase modulate their internal signals; this is very efficient because the signal is always present at the multipliers. A microwave phase modulator switches the phase by 180° at a 1.5 kHz rate, a compromise between noise level and switching overheads. We retain the most significant 16 bits from the ADC. A conversion of 7.33×10^{-7} A/V between the multiplier and ADC, 11.5 ms integration time, and ADC maximum input charge of 250 pC results in electronic noise at the 1–2 bit level. Matching 1 bit of quantization to the rms of Gaussian-distributed noise is just fine enough to eliminate correlation between the quantization error and the input signal, permitting accurate digital integration. Allowing 14 bits of ADC range for the input signal's minimum level, the input signal can increase by about another factor of 4 (6 dB) at most for calibration and other level changes. An adjustable attenuator at the spectrometer's input accommodates a wider range of power levels. We set the spectrometer's signal level by increasing the input power until radiometric noise increases the readout variance in the lags which have little correlated signal by a factor of 10–15. At this level the receiver noise dominates the total instrumental noise, with the spectrometer's electronic noise contributing only a few percent to the total at most.

Each board carries 16 multipliers and the associated electronics. Most of the board's upper surface area is taken up by the individual preamplifiers, demodulators, and analog-to-digital converters. Small amounts of space are also needed for an active low-pass filter for the multiplier power supply (the multiplier passes noise on its supply voltage to its output with only little attenuation), ADC voltage reference, temperature sensor, and digital interfaces. The multipliers, tap components, and delay lines occupy the center part of the board's bottom side. The boards can be cascaded easily, with timing and control signals fed to all boards in parallel and the data from the ADCs daisy chained into one long serial string. Differential line drivers and receivers handle fast signals, with simple buffers for slow signals (e.g., ADC setup strings).

Physically, the boards are four layer hybrids of microwave⁸ and FR-4 materials, providing both good microwave and mechanical performance. Nearly all of the components on the boards are in surface-mount packages, permitting a small board that fits in standard chassis: 3U (100 mm) high by 10 in. long. Fields from the microstrip lines are well contained in the board material, and objects more than 5 mm from the line have little influence on the coupling along the lines. Synchronous detection and correlation in time along the lines reduces pickup along the lines to negligible levels,

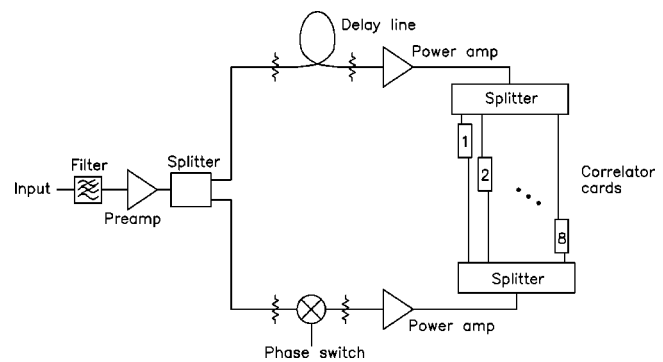


FIG. 2. Schematic overview of WASP2's overall signal path. The autocorrelation function is produced by splitting the input into two streams and cross-correlating these signals. Eight correlator cards, appropriately spaced in time by cable delays, have a total of 128 lags.

so shielding enclosures around the transmission lines are not necessary. This reduces fabrication complexity and eliminates potential enclosure resonances.

B. System layout

WASP2 obtains its 128 lags by combining signals from eight correlator cards. Figure 2 is an overview schematic signal path for WASP2. The input signal is split into two counter-propagating streams and is then correlated. Autocorrelation functions are symmetric in time delay (lag), so measurement of only the positive lags is necessary; an additional cable delay in one arm puts the zero-delay point near one end of the correlator string. It is prudent to extend the range of lags slightly into the negative delays to insure an accurate measurement of the zero-delay fringe. This "white-light" fringe need not precisely coincide with a particular lag, but it must be bracketed by spectrometer lags.

The spacing between multipliers is shorter than typical microwave connector and other interconnection lengths, so correct spacing of the first multiplier of one board from the last multiplier of the preceding board requires at least two staggered strings of multipliers. Delay line cables with stepped lengths put each card at the appropriate time delay (right side of Fig. 2). Broadband amplifiers⁹ with 1 dB compression points near +22 dBm drive the strings through eight-way splitters, which isolate the cards and minimize power variations along the strings. A small amount of saturation in these amplifiers is the main source of nonlinearity for the spectrometer. Since the amplifier gain compresses quite uniformly across the band, the dominant effect is a slight and predictable underestimate of the spectral power scale.⁶

The correlator card gain is quite flat with frequency, with most of the bandpass shape produced by the microwave components (the double-balanced mixer¹⁰ we use for the 180° phase switch produces most of the shape). Figure 3 compares the gains of the correlator card, spectrometer, and microwave components. The correlator board is essentially flat to 2000 MHz, with a +1 dB gain bump near 2500 MHz and -3 dB rolloff near 4000 MHz. At low frequencies, the correlator boards should respond well down to frequencies below 100 MHz, where the dc blocking capacitors begin to

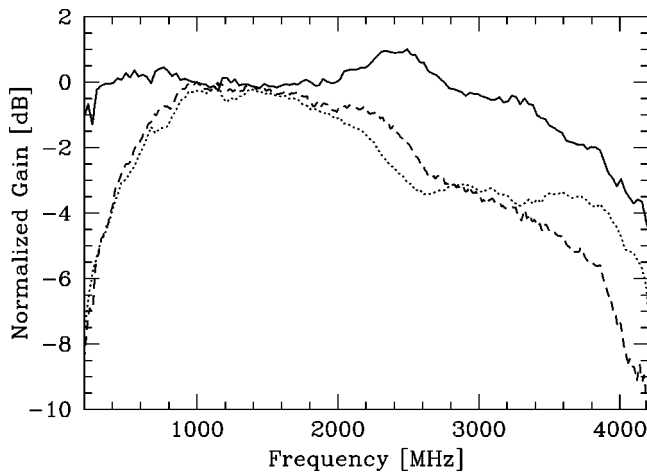


FIG. 3. WASP2's correlator board passband (solid line), the overall spectrometer response (dashed line), and the gain of the microwave processing components (dotted line). The correlator board gain passband was obtained by dividing the spectrometer's gain derived from phase calibration measurements by the microwave components' gain measured with a network analyzer.

have significant impedance and the reflections from all the taps again begin to pile up in phase. The present microwave electronics produce a 6 dB system bandwidth of 3600 MHz, from 280 to 3880 MHz. A gain equalizer can compensate for much of the structure introduced by the microwave components, with this task considerably simplified by moving the phase switching to an octave band or narrower before conversion to the correlator board's multioctave band.

An anti-aliasing filter at the input cuts off power above f_c . As a compromise between band flatness near the filter's edge and aliasing, a small band (~ 60 MHz) of high frequencies is allowed to weakly alias into the highest one or two spectral channels. A small amount of aliasing here is not a practical problem since the highest few spectral channels usually contain some edge effects and are discarded.

An Intel 80C251SB microcontroller manages the spectrometer's real-time tasks. This 8 bit microcontroller with a 16 MHz clock accumulates the data from the spectrometer ADCs, sends TTL-level signals to the telescope's chopping secondary and beamswitch ("nodding") inputs, and sets the spectrometer's instrument state. The code is written in C, compiled,¹¹ and downloaded to flash memory on the microcontroller board. The microcontroller, its memory, and RS-232 and RS-485 serial interfaces are on a small commercial board¹² which mounts on a 3U circuit board in the chassis that also carries associated interface and clock circuitry. A hardware clock drives the ADC readouts at a constant rate, so the physical state of the spectrometer is the same whether it is integrating on source or not. On a request over its serial interface from the host computer to begin an integration, the microcontroller synchronizes its data acquisition to the spectrometer clocks and accumulates data. When the accumulation cycle has finished, the microcontroller sends the data to its PC or workstation host over the same serial interface for further processing. Transferring the accumulated 256 4-byte words (128 lags in two "nod" positions) takes about 0.5 s at 19.2 kbaud.

The correlator cards, microcontroller board, microwave electronics, and other support electronics mount within a 4U (7 in. high) chassis. Although the circuit boards are 3U high, it is convenient to have extra vertical space in the chassis for the eight-way splitters and coiled delay line cables. Altogether, the chassis contains about 14.5 m of delay cable: each card sits in the middle of 1.6 m of cable, and the delay compensation is essentially the same length. A separate chassis contains the power supplies: ± 5 V for the correlators, microcontroller, and support electronics, and +15 V for the microwave amplifiers. Individual correlator cards dissipate 4.5 W and the entire spectrometer dissipates 40 W.

III. RECOVERING THE SPECTRUM

Although the delay times to each multiplier are accurately established by cable lengths and the signal tap positions along the microstrip lines, small fabrication and frequency-dependent component variations add small delay irregularities. Irregular sampling is not fundamentally inferior to regular sampling; it is just more difficult to treat theoretically. Inverting the autocorrelation function to obtain the spectrum is complicated by this irregular sampling along the lines, and a simple Fourier transform would produce a distorted spectrum. Rewriting the transform for an analytical solution is possible when the time delay is a separable function of length and frequency (e.g., uniform sampling on dispersive lines). Each of WASP2's lags has a slightly different frequency dependence, however, and length and frequency effects are not separable functions.

Our transformation from the autocorrelation function to power spectrum still relies on the basic principle of Fourier transforms and series: any signal may be decomposed into a family of appropriate monochromatic signals. Calibration with an appropriate family of monochromatic signals completely establishes the spectrometer's response (Fig. 4). Any autocorrelation function will be a linear superposition of calibration autocorrelation functions if the spacing between calibration signal frequencies is equal to the Nyquist corner frequency of the spectrometer divided by the number of lags, or finer. Finding the spectrum of an unknown signal involves decomposing its measured autocorrelation function into a weighted sum of the known calibration functions; the power at each frequency is proportional to its weight in the sum.

The decomposition is straightforward. Starting with the case of a finite number of lags and a continuous range of frequency, and neglecting constant unit conversion factors, a spectral density $S(f)$ produces a voltage v_i at lag number i of

$$v_i = 2 \int_0^{\infty} S(f) k_i(f) df, \quad (4)$$

where $k_i(f)$ is the response function of lag number i . [The response functions for an ideal correlator are the usual Fourier transform kernels $k_i(f) = \cos(2\pi\tau_i f)$.] It is convenient to discretize the integral and use matrix notation for the transformation between power spectrum and correlation function. With the input and output signals represented by row vectors,

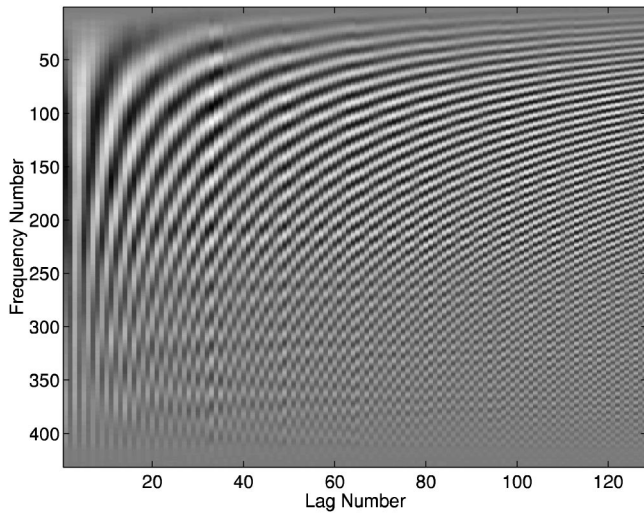


FIG. 4. An image of WASP2's calibration data. The intensity shows the signal's strength. The y axis shows steps in calibration frequency, with 431 samples from 100 MHz (long wavelength correlation functions) at the top to 4400 MHz (short wavelengths) at the bottom. The nearly vertical bright fringe near lag 3 is the zero time lag position. Vertical structure near lag 35 shows multipliers with slightly higher responsivity than the others. Phase discontinuities between the eight 16 lag boards would appear as vertical structures at lags near multiples of 16 but are not present at a significant level. Passband gain changes cause the intensity modulation from top to bottom.

$$\mathbf{v} = \mathbf{s}\mathbf{K}. \quad (5)$$

The voltage output vector \mathbf{v} has M elements, one for each lag; the elements of the spectral vector \mathbf{s} represent power at N discrete frequencies; and the transformation matrix \mathbf{K} is $N \times M$. A family of monochromatic signals with unit power is represented by the family of vectors containing delta functions in frequency: $\mathbf{s}_1 = (1, 0, 0, \dots, 0)$, $\mathbf{s}_2 = (0, 1, 0, \dots, 0)$, and so forth. This ordering of frequencies is not fundamental but will prove convenient. Measurements of N of these row vectors can be easily handled by combining them in an $N \times N$ array

$$\mathbf{S} = \begin{bmatrix} \mathbf{s}_1 \\ \mathbf{s}_2 \\ \vdots \\ \mathbf{s}_N \end{bmatrix} = \begin{bmatrix} 1 & 0 & 0 & \dots & 0 \\ 0 & 1 & 0 & \dots & 0 \\ & & \vdots & & \\ 0 & 0 & 0 & \dots & 1 \end{bmatrix}. \quad (6)$$

The set of output voltages is then another array of vectors with M lag elements at N frequencies

$$\begin{bmatrix} \mathbf{v}_1 \\ \mathbf{v}_2 \\ \vdots \\ \mathbf{v}_M \end{bmatrix} = \begin{bmatrix} \mathbf{s}_1 \\ \mathbf{s}_2 \\ \vdots \\ \mathbf{s}_N \end{bmatrix} \mathbf{K} \quad \text{or} \quad \mathbf{V} = \mathbf{S}\mathbf{K}. \quad (7)$$

Given a known set of \mathbf{S} and measured voltages \mathbf{V} , it is simple to solve for the transform, \mathbf{K} :

$$\mathbf{K} = \mathbf{S}^{-1}\mathbf{V}. \quad (8)$$

By stepping in increasing frequency as in Eq. (6), $\mathbf{S} = \mathbf{I}$, the unit matrix, which is its own inverse and drops out of the right hand side of Eq. (8). This leaves \mathbf{K} equal to the measured outputs \mathbf{V} without further calculation. If necessary, frequency-dependent shape in the calibration source can be

accounted for in a separate diagonal matrix which includes bandpass shapes. Calibration with monochromatic signals of even arbitrary amplitude is important for establishing the spectrometer's internal phase behavior, but the amplitude response can be separately calibrated with broadband loads.

Once \mathbf{K} has been found, it is possible to recover the unknown spectrum from the observed voltages at each lag,

$$\mathbf{s} = \mathbf{v}\mathbf{K}^{-1}. \quad (9)$$

In practice, we oversample in frequency during the spectrometer's calibration, covering a very wide band with frequency spacing a few times finer than the spectrometer's resolution. It is necessary to make calibration measurements at all frequencies where the spectrometer electronics have any significant response. Otherwise, the spectral recovery will alias signals that are outside the calibration band but are still within the spectrometer's response band: it can only assign components of the autocorrelation function to the measured frequencies in the calibration.

Since WASP2's basis functions are overconstrained by our measurements the matrix \mathbf{K} contains some redundancy and cannot be trivially inverted. We invert this matrix using singular value decomposition,¹³ keeping about 90% of the vectors. In spectra, the "missing" vectors correspond to frequencies where the microwave gain is low, so no information is lost within the spectrometer band. Increasing the number of discarded vectors begins to noticeably eliminate signals that appear in low-gain parts of the main spectrometer band. Decreasing the number of discarded vectors increases the amount of power scattered across the baseline by residual statistical and numerical noise from the inversion of a nearly singular matrix. The spectra produced with this scheme are as overresolved as the calibration, so only spectra smoothed or binned back to at least the frequency resolution set by the sampling theorem have a unique meaning.

IV. PERFORMANCE

A. Spectra

Figures 5, 6, and 7 are sample spectra taken with WASP2 in the laboratory and at the Caltech Submillimeter Observatory's (CSO's) 10.4 m diam radio telescope. Figure 5 is typical of monochromatic spectra from data taken for the spectrometer calibration. The "ringing" to either side of the line is the usual result of truncating the correlation function, which still has large amplitude at high lags for a narrowband signal. The magnitude and phase of the structure agrees very well with simulations of the ideal response. Ringing tends to average away for wide lines, and smoothing or binning (apodization of the autocorrelation function) will reduce the ringing at the expense of spectral resolution. Figure 6 is a spectrum of a noise source with a 1000 MHz bandpass filter that shows the spectrometer's broadband response. The spectrum was taken with the spectrometer mounted at the cassegrain focus of the CSO's telescope and has been divided by the spectrum of the noise source without the filter. Figure 7 is a spectrum of the carbon monoxide $J=3-2$ transition from the starburst galaxy M82 taken with WASP2 and the CSO's facility 345 GHz receiver. The receiver has a 1000

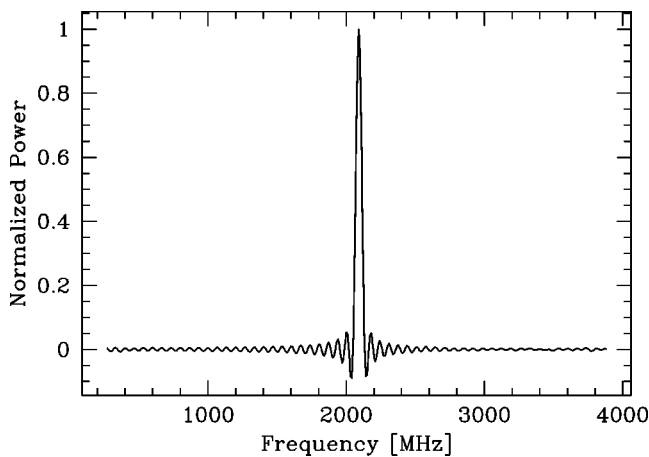


FIG. 5. Spectrum of a typical monochromatic signal. The ringing on both sides of the line is caused by the abrupt truncation of the autocorrelation function and matches theory. Ringing is less pronounced for broad spectral lines, whose autocorrelation functions tapers smoothly to low values at high lag.

MHz bandwidth, so the line fills only a fraction of WASP2's band. WASP2 is designed for observations of active galaxies in the short submillimeter CO $J=6-5$ transition near 691.5 GHz with the SURFER extragalactic receiver.¹⁴ With SURFER's 4–8 GHz IF bandwidth, a 691 GHz spectrum would cover about 1500 km s^{-1} with 11 km s^{-1} velocity resolution.

B. Stability

Stability is a paramount concern for spectrometers, and WASP2's electronics have proved to be suitable for the long integration times common in radio astronomy. Offset drift, which is usually the dominant problem for analog systems, is largely removed by the layers of internal phase switching within WASP2. Small fluctuations in multiplier bias voltage can appear as an offset in the autocorrelation function's voltage, but each board's active low-pass multiplier bias filter gives these fluctuations a much longer time constant than the phase switch switching time. Low-pass filtering, rather than

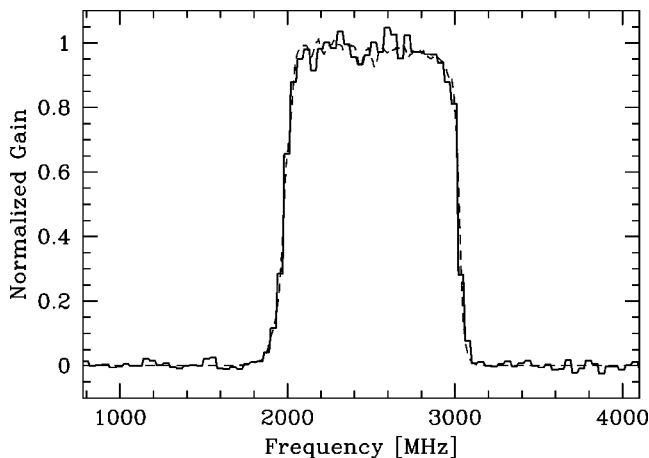


FIG. 6. Spectrum of a noise source through a 2000–3000 MHz bandpass filter, divided by the spectrum of the noise source without the filter. The noise source limits the spectrum to frequencies above 800 MHz. For comparison, the light dashed line is the filter's response measured with a network analyzer.

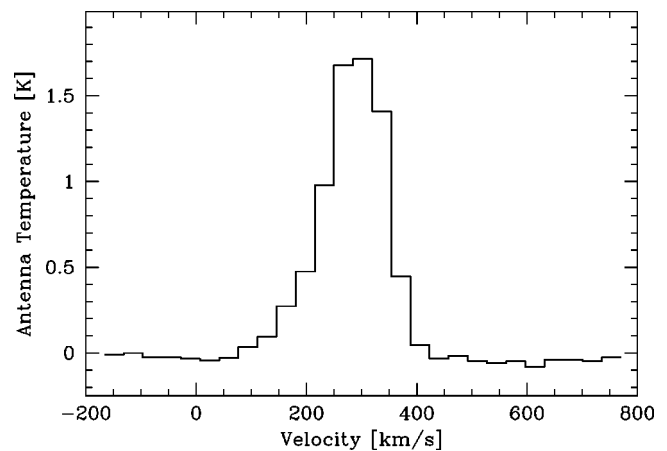


FIG. 7. Spectrum of the starburst galaxy M82 taken with WASP2 and the CSO 345 GHz facility receiver. The spectrum covers the receiver's entire 1000 MHz bandwidth with 40 MHz (35 km s^{-1}) resolution. No baseline corrections have been made. The integration time was 12.16 min with a 1 Hz sky chop frequency.

voltage regulation, leaves any residual common to all boards in the spectrometer. A common offset would transform to a δ function at zero frequency without affecting the spectra in band. Since the microwave frequency calibration does not include zero frequency, the offset appears in the low-response parts of the band that are not properly recovered.

Gain drift is a problem for all receivers and spectrometers, but has little effect when the drift is small over typical switching times. WASP2's amplifiers are thermally insulated and mounted on thick aluminum plates for long time constants. The spectrometer's overall total power stability is good, with typical peak-to-peak drifts of a few tenths of a percent ($\sim 0.01 \text{ dB}$) over minutes once temperatures have stabilized. We use Allan variance measurements¹⁵ to characterize stability over a range of time scales. In the absence of microwave power, individual channels show white noise past tens of seconds. With power applied, the total power lag shows a transition from white noise to $1/f$ noise or drifts at a timescale of a few seconds. Samples at slightly longer lags, which are sensitive to a combination of total power and band shape change, do not show any change in noise spectrum with applied microwave power.

A potentially important temperature effect is a change in phase velocity along the transmission lines. Length changes between calibration and observation will scatter power across the spectrum, increasing the apparent noise level. To understand this effect, start with an autocorrelation function modified by small changes in lag times, $R(\tau')$, then expand to first order in a Taylor series of $R(\tau)$ with no lag errors and a lag error term $\theta(\tau)$:

$$R(\tau') = R[\tau + \theta(\tau)] \approx R(\tau) + \theta(\tau) \frac{dR(\tau)}{d\tau}. \quad (10)$$

Fourier transformation shows that the power spectrum is

$$S(f') \approx S(f) + \text{Re}\{j2\pi f [\Theta(f) * S(f)]\}, \quad (11)$$

the error is an additive term proportional to a frequency-scaled convolution of the true power spectrum $S(f)$ with the odd part of the error function's Fourier transform. Small er-

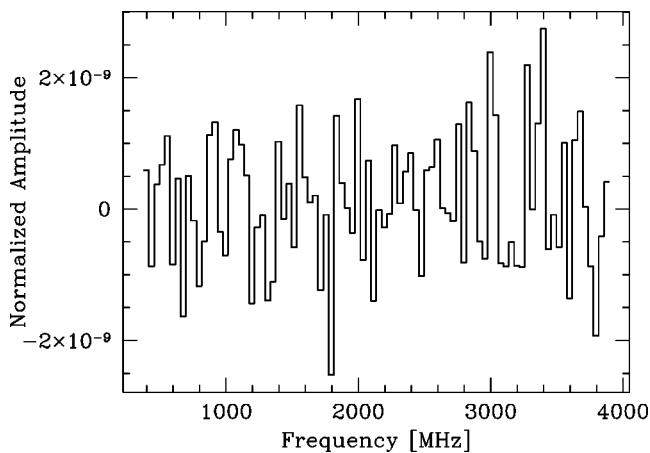


FIG. 8. Spectrum of a laboratory noise source after a 40 h chopped and noded integration. The spectrometer input power was typical for normal observations; the amplitude scale is normalized by this average input signal level. The spectrum may show a slight tilt, but there is no sign of the system bandpass.

rors in the reconstruction produce spurious structure that is proportional to the intensity of the uncorrupted spectrum. This affects the dynamic range of individual spectra rather than adding a constant amount of excess noise to all spectra, and weak spectra are not disproportionately affected by phase errors from temperature changes.

Effects from phase errors are reasonably small over a useful range of temperatures. For a typical midband monochromatic signal, a temperature change of 5 °C produces additional baseline ripple with a peak amplitude $\pm 0.5\%$ of the peak value. The delay change is linear along the transmission lines, with the largest changes on the circuit boards, and the effect could be removed in software if needed.

A laboratory test shows that WASP2 integrates stably for many hours. For this test a noise diode and amplifier provided an approximately constant signal with an average power level typical of normal spectrometer operation. The amplitude scales in the measurements were normalized to this average value of the unchopped spectrum. Since the test signal was essentially constant, chopping and nodding should produce a signal with zero amplitude within noise across the spectrum. Figure 8 shows that the baseline is close to zero amplitude and is essentially featureless after 40 h of chopped and noded integration. Of most importance, neither passband structure from the noise source nor from the microwave components appear in the spectrum. Figure 9 shows the root-mean-square (rms) variation across the spectrum for individual 8 min integrations and the rms across the progressively accumulated spectrum. The rms of the accumulated spectrum varies somewhat with time but integrates down as the square root of time within statistical error. It is likely that gain instabilities in the atmosphere or receiver and intermediate frequency chain will dominate the system stability.

C. WASP2 in operation

WASP2 demonstrates that analog correlators are a practical and attractive approach for wideband spectroscopy with moderate resolution. WASP2 covers a contiguous bandwidth

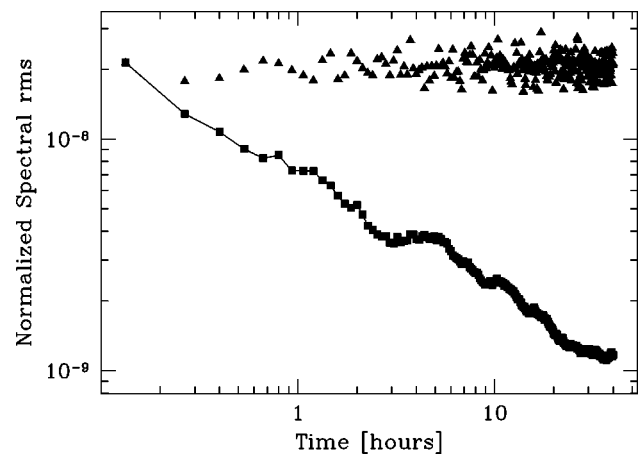


FIG. 9. Root-mean-square noise across spectrum for individual spectra (squares) and the accumulated spectrum as a function of time (triangles) for chopped and noded integration on a laboratory noise source. The spectrometer input power was typical for normal observations; the amplitude scale is normalized by this average input signal level. The rms spectral noise integrates down as $t^{-0.5}$ for the 40 h length of this trial.

two to three times larger than other spectrometers, a considerable advantage because it eliminates structure caused by stitching together small subbands. WASP2 is stable, compact, and requires little power. These properties make it practical to mount the spectrometer very close to the receiver on the telescope. A short and rigid connection between receiver and spectrometer improves spectral baselines by eliminating cable flexure and severe gain slopes over large bandwidths from long interconnecting cables. In addition to WASP2's strengths, we have carefully explored many of the low-level effects that plague any instrument. We find none that are significant problems; this an excellent instrument for wideband astronomical spectroscopy.

ACKNOWLEDGMENTS

P. Teuben, K. G. Isaak, and J. Morgan have made essential contributions to the work described here. J. Ward, R. Baum, J. Staguhn, C. Holler, and J. Gottshalk have also made valuable contributions to spectrometer developments and use at the telescope. The authors thank T. G. Phillips and the staff of the Caltech Submillimeter Observatory for their support of this project. The staff of Protocircuits of Florida and Taconic ADD have been generous with advice and samples of board material. Financial support for parts of this work has been provided by NASA Grant No. NAG5-6044, NSF Grant No. AST-9819747, USRA funds for SOFIA heterodyne spectroscopy, and by the University of Maryland.

¹A. I. Harris, K. G. Isaak, and J. Zmuidzinas, Proc. SPIE **3357**, 384 (1998).

²We identify components and manufacturers to fully describe the instrument. Alternatives exist for many components and may be superior to the devices we chose; our identification is not a recommendation or endorsement.

³Technical Research and Manufacturing Co., <http://www.trm.com>, models DMS 825 and DMS 225.

⁴Agilent Technologies, <http://www.agilent.com>.

⁵B. Gilbert, IEEE J. Solid-State Circuits **3**, 365 (1968); J. Wholey, I. Kipnis, and C. Snapp, IEEE MMWMC Symposium Digest, Long Beach, CA, 1989, p. 281.

- ⁶A. I. Harris, Berkeley-Illinois-Maryland Array Memorandum Series #80, available at [http://bima.astro.umd.edu/memo/\(2000\)](http://bima.astro.umd.edu/memo/(2000)).
- ⁷Burr-Brown, <http://www.bbrown.com>, charge integrating 20 bit analog-to-digital converter model DDC101U.
- ⁸Taconic Advanced Dielectric Division, <http://www.taconic-add.com>, RF-35 ceramic filled teflon/woven glass laminate.
- ⁹Cougar Components, <http://www.cougar.com>, model A2CP5121.
- ¹⁰Watkins-Johnson model M1G.
- ¹¹Keil Software, Inc., <http://www.keil.com>, μ Vision Integrated Development Environment.
- ¹²Phytec America LLC, <http://www.phytec.com>, microModul 251.
- ¹³W. H. Press, B. P. Flannery, S. A. Teukolsky, and W. T. Vetterling, *Numerical Recipes*, (Cambridge University Press, Cambridge, 1986), pp. 52–64.
- ¹⁴J. Ward, D. Miller, J. Zmuidzinas, P. O'Brien, H. G. LeDuc, and R. Bicknell-Tassius, Proceedings of the Eleventh International Symposium on Space Terahertz Technology.
- ¹⁵D. W. Allan, Proc. IEEE **54**, 221 (1966); G. Rau, R. Schieder, and B. Vowinkel, Proceedings of the 14th European Microwave Conference, 1984, p. 248.